Nuclear Instruments and Methods in Physics Research A 800 (2015) 29–33

Contents lists available at ScienceDirect

Nuclear Instruments and Methods in Physics Research A

journal homepage: www.elsevier.com/locate/nima

Thick target double differential neutron energy distribution from $^{12}C+$ ^{27}Al at 115 MeV

V. Suman [a], C. Sunil [a,*], Soumya Nair [a], S. Paul [a], K. Biju [a], G.S. Sahoo [a], P.K. Sarkar [b]

[a] Health Physics Division, Bhabha Atomic Research Centre, Trombay, Mumbai 400085, India
[b] Manipal Centre for Natural Sciences, Manipal University, Manipal 576104, India

ARTICLE INFO

Article history:
Received 4 June 2015
Received in revised form
20 July 2015
Accepted 1 August 2015
Available online 11 August 2015

Keywords:
Thick target neutron yield
Neutron spectrum
Time of flight
FLUKA
PACE
Heavy ion reaction

ABSTRACT

Neutron yield from 115 MeV ^{12}C projectiles bombarding a thick ^{27}Al target has been measured using the time of flight technique. Nuclear reaction model code PACE and the FLUKA Monte Carlo code are used to calculate the yield and the results are compared with the experimental data. The energy for maximum neutron emission in experimental measurement and reaction code output has a slight disagreement in the extreme forward emission angle but in all other angles it has a close match. The slope of the distribution in general shows good match between the experimental and the reaction code results as well as FLUKA calculations. The maximum energy of the emitted neutrons is observed to decrease with the increasing emission angles.

1. Introduction

For accelerator radiation protection, the starting point is the characterization of the radiation source term, usually expressed in a radiation protection unit such as the ambient dose equivalent ($H*(10)$) at a given angle with respect to the beam direction [1]. They are usually obtained by measurements using techniques/instruments such as conventional rem counters, track etch detectors, proton recoil techniques etc., or are computed using simple empirical techniques, standalone nuclear reaction model codes that can calculate the emission cross section, or by radiation transport codes that have various nuclear reaction models incorporated. In ion accelerators, neutrons are the major prompt radiation. Measuring neutron $H*(10)$ with a conventional dose equivalent meter (rem counters) has its share of uncertainties in the form of energy response of the instrument. The primary invariant quantity required for estimating the ambient dose equivalent, obtained either by measurement or by computation, is the energy spectra of the radiation under consideration at various angles of emission with respect to the beam direction. In the case of neutrons, the source term, when described in terms of the hardness of the energy spectrum, the differential (in energy and solid angle) and integral yields and their angular distribution, will result in easy computation of the unshielded dose rates, help frame empirical relations, determine the effective attenuation lengths of shielding materials and serve as a starting point for shielding and activation calculations using Monte Carlo radiation transport codes. While it is advisable to use experimental data as far as possible, the dearth of it necessitates the use of empirical techniques or reaction model codes. It is therefore important to study the effectiveness of such techniques and to understand any major deviations in their results when compared to experimental data.

The thick target neutron yield data from heavy ion reactions are very few in the energy range of ~10 MeV/A [2–6]. However, no experimental data has been reported for this system at 115 MeV [7]. The importance in studying the yield from thick targets, which stop the projectiles completely, is because it represents the accidental or intentional beam loss scenarios in an accelerator facility which produces the radiation that needs to be shielded. It is also a cause for secondary cancer induction in proton and heavy ion therapy as the secondary particles that are produced during the treatment, either from the passive scattering devices or from the tumor itself, will irradiate the healthy tissues. Estimating these quantities will require the understanding of the physics of the reaction for effective implementation in the Monte Carlo code such as FLUKA [8,9], which has the intranuclear cascade, pre-equilibrium and evaporation models built in to calculate the particle yields. At higher energies, the intranuclear cascade is the dominant mode of interaction. As the projectile energy reduces, pre-equilibrium (PEQ) emission begins to be important. At 10–15 MeV/amu and lower, PEQ is on the wane while the compound

* Corresponding author. Tel.: +91 22 25592012.
E-mail addresses: csunil11@gmail.com, sunilc@barc.gov.in (C. Sunil).

http://dx.doi.org/10.1016/j.nima.2015.08.007
0168-9002/

nucleus (CN) evaporation process is on the rise. It is important to know this transition point as the models that handle the PEQ and CN are different. Invoking them at the correct energy will result in a better prediction of the slope of the spectrum (hardness) and the overall yield. Testing of such models and the transition point require a large set of experimental data.

Here we report the experimental double differential neutron yield from 115 MeV ^{12}C (~9.6 MeV/amu) ions incident on a thick Aluminum target. The results are compared with the values obtained from the calculations using the nuclear reaction code PACE [10] and the FLUKA Monte Carlo code.

2. Experimental method

The experiment was carried out at the Linac extension of the Pelletron Accelerator facility BARC-TIFR, Mumbai, India. Carbon ions of 115 MeV were incident on a thick hemispherical shaped aluminum target of 3 mm thickness and 40 mm diameter. The thickness in all directions was more or less the same and was such that the neutrons do not undergo significant scattering and attenuation before reaching the detector. Calculations using the FLUKA code for 1 MeV neutrons indicate an attenuation of 5% and 8% at 3 mm and 5 mm thicknesses respectively. The attenuation is lower as the energy increases. The ions were completely stopped in the target since their range in Al is approximately 0.2 mm as calculated by the SRIM code [11]. The emitted neutrons were measured using five EJ-301 (5 cm × 5 cm, Scionix Holland) liquid scintillation detectors, kept at a distance of 1.5 m at angles 0°, 30°, 60°, 90° and 120° with respect to the beam direction. To account for the background contribution from the scattered neutrons from the nearby structural materials, shadow bar correction was carried out for individual detectors. Here, an iron bar of diameter 5 cm and length 30 cm was kept followed by high density poly-ethylene (HDPE) of same dimensions in the line of the target and the detector. The high energy neutrons undergo inelastic scatterings in the iron bar, gets reduced in energy and undergo elastic scattering in the hydrogen rich HDPE before finally getting captured. Such an arrangement (Fig. 1) cuts off almost all the direct neutrons and only the scattered component are counted. The net counts from the direct neutrons were then obtained by subtraction. The target was electrically isolated and a precision beam current integrator (ORTEC make) was used to measure the total charge incident and thus the number of projectiles incident on the target.

The energy distribution of the emitted neutrons was measured using time of flight (ToF) technique while the pulse shape discrimination (PSD) method [12], was used to separate neutrons from photons. The anode output from the detector photo multiplier tube was given into a multi parameter discriminator (MPD-4, Mesytec) input. One channel of the MPD-4 gives three outputs (pulse height, pulse shape timing information (PST) and a logic gate signal) for every input. The gate obtained from each detector was split into two, and one from all the detectors were used in OR logic mode to generate a master gate for acquisition purpose. The second gates were used as start signal to the ToF time to amplitude converter (TAC, Canberra make). The stop signal for the ToF-TAC was drawn from the RF output of the buncher which signals the arrival of the beam bunch at the target. The full width at half maxima (FWHM) of the bunch was less than 1 ns as measured by a BaF_2 detector that was placed close to the target. The amplitude of the output from the ToF-TAC corresponds to the flight time of the event registered, either by photons or neutrons. Three parameters were drawn from each detector (fifteen in total) and fed to ADC (analog to digital converter) for acquisition in list mode. A simplified block diagram of the electronic setup used in the experiment with a single detector is shown in Fig. 2. The PST and ToF-TAC outputs obtained are shown in Figs. 3 and 4 respectively. The n–γ separation can be seen to be good and has a figure of merit (FOM, defined as the ratio of the separation of the peaks to the sum of the full widths at half maximum) close to 1.2. A two-dimensional plot was constructed using these two parameters and one such plot is shown in Fig. 5. When PST and ToF are used together, excellent n–γ separation is obtained as is seen in the figure. Software gates were then used to select the neutrons in an offline analysis. The flight information of neutrons was obtained from the TAC calibration factor and the position of the prompt gamma peak. This was converted to neutron energy, grouped in

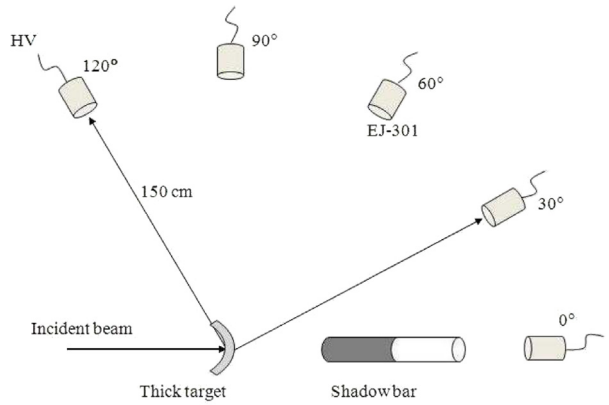

Fig. 1. Pictorial representation of the experimental arrangement used.

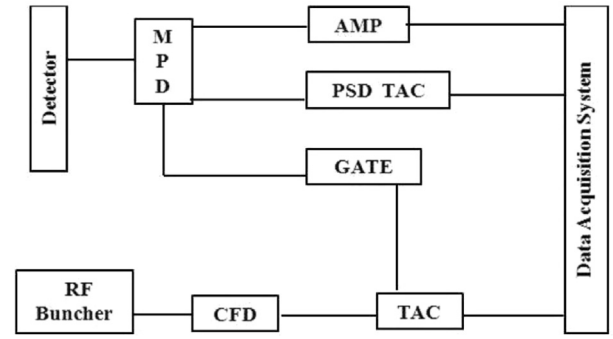

Fig. 2. Simplified block diagram for the electronics used for data acquisition (shown for one detector).

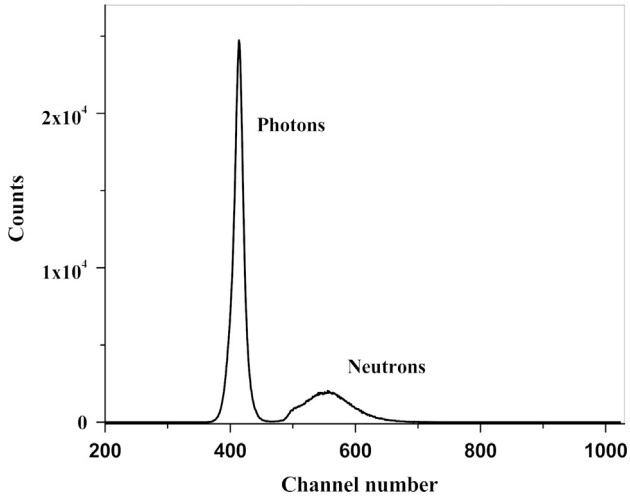

Fig. 3. Measured one dimensional pulse shape discrimination spectrum showing time separation for photons and neutrons.

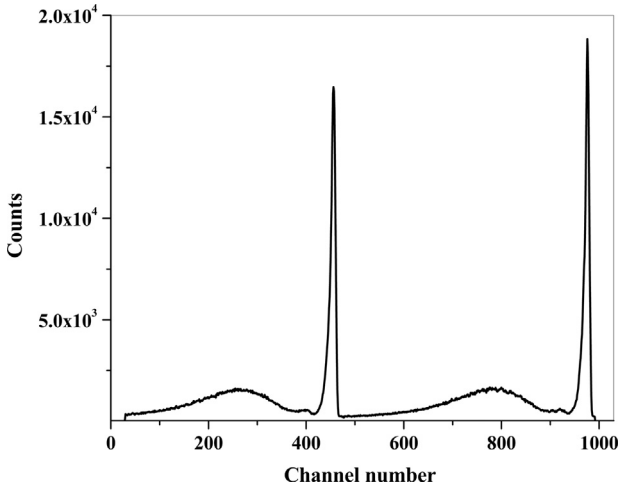

Fig. 4. Neutrons and photons seen in one dimensional time of flight spectrum corresponding to two bunches of beam.

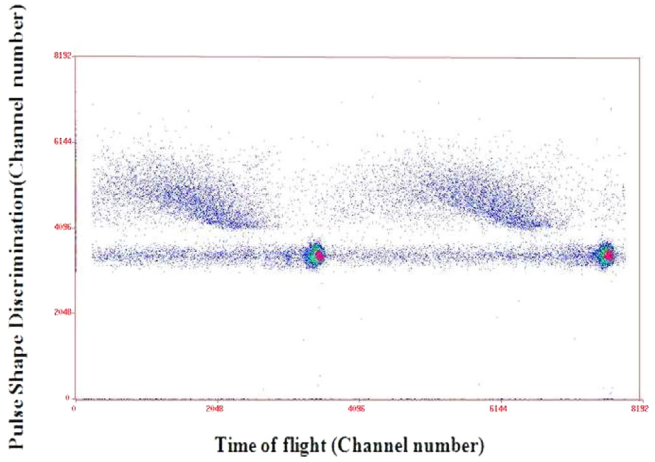

Fig. 5. Two dimensional plot of the measured time of flight and pulse shape discrimination spectra showing neutrons separated from photons.

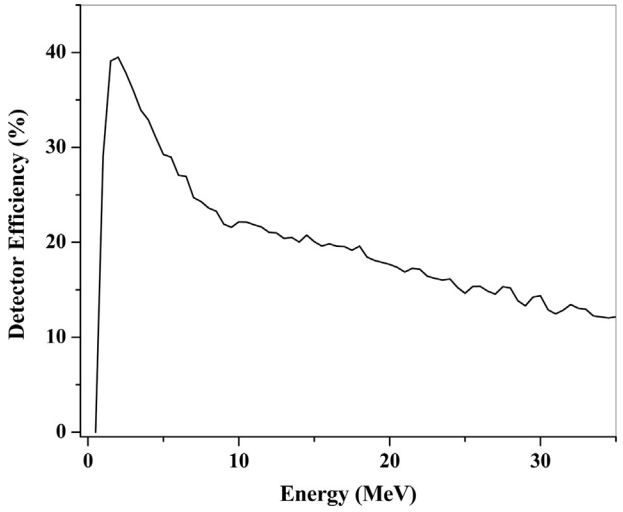

Fig. 6. Efficiency plot for detector EJ-301, obtained from Monte Carlo simulations.

0.5 MeV bins, corrected for the energy dependent detector efficiency, solid angle and the total number of projectiles incident on the target. The intrinsic detector efficiency (Fig. 6) was obtained using Monte Carlo calculations [13] and was assumed to be same for all the five detectors.

3. Uncertainty in energy

The relative energy resolution, for the neutron energies obtained by the ToF method is given [14] as follows:

$$\frac{\Delta E}{E} = \gamma(\gamma+1)\left(\frac{\Delta t}{t}\right)$$

$$\gamma = 1+\frac{E}{Mc^2}$$

where E is the neutron kinetic energy, M is the neutron rest mass, Δt is the overall time resolution and t is the neutron time of flight. The factors contributing to Δt are the inherent time resolution of the neutron detectors, the time spread in the beam bunch, time dispersion arising due to energy spread in the incident beam ($\sim \pm 0.5$ MeV), time spread in the production of neutrons due to finite thickness of the target and the time spread arising due to finite thickness of the scintillation detector. The uncertainties arising due to finite thickness of target will be negligible since target thickness is small (3 mm). Thus the total time resolution Δt can be approximated as follows:

$$\Delta t = \left[(\Delta\tau)^2 + \left(\frac{\Delta x}{v}\right)^2\right]^{0.5}$$

where $\Delta\tau$ is the summed time dispersion of the scintillator detector and the prompt gamma spread, the latter being proportional to the beam bunch spread. Δx is the finite thickness of the detector and v is the velocity of the incident neutron. $\Delta\tau$ is taken as the FWHM of the prompt gamma peak in the neutron ToF spectra and in the present measurement it was less than 1 ns.

4. Experimental uncertainties

The experimental uncertainties are mainly categorized as normalization uncertainty which has contribution from the pulse pile up leading to detector dead time, uncertainty in the solid angle and in the flight path length. The dead time was $\sim$5% while the uncertainty in the solid angle and the flight path length were $\sim$2%. The uncertainties in the measured total charge beam due to the current integrator was less than 1% while the uncertainty in the Monte Carlo calculations of the detector efficiency was less than 2%. The statistical uncertainties in the total counts were less than 5% in forward directions (0° and 30°, 60°) and $\sim$10% in the backward angles (90° and 120°).

5. Model calculations

Nuclear reaction model code PACE and FLUKA Monte Carlo radiation transport code are used to analyze the experimentally observed results.

5.1. PACE

The Projection Angular-momentum Coupled Evaporation (PACE) code uses Monte Carlo technique to simulate the decay of compound nuclei through the various available decay channels. The possible decay channels are considered randomly according to their respective probabilities. Transmission coefficients for light particle (n, p) evaporation are obtained by optical model calculations. Angular momentum projections are calculated at each stage of de-excitation to determine

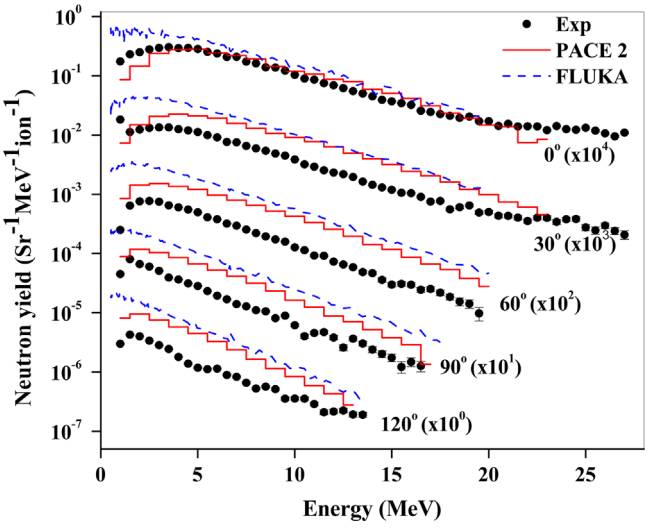

Fig. 7. Double differential neutron yield for thick target obtained from experiment plotted in comparison to PACE and FLUKA results.

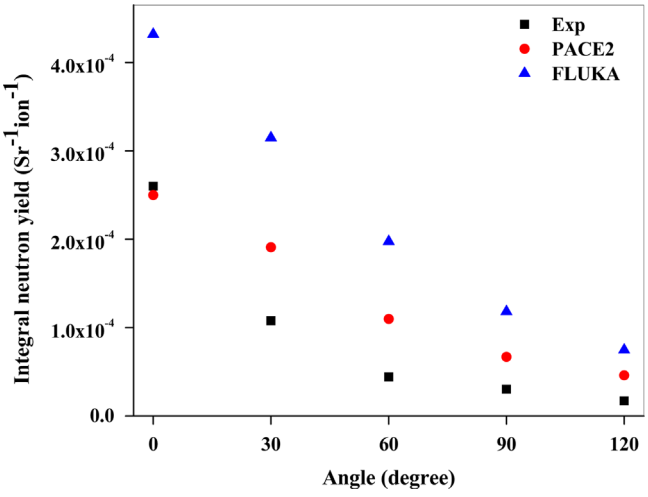

Fig. 8. Energy integrated neutron yield obtained from experimental measurements compared with calculated results.

the angular distribution of emitted particles as functions of angle around the recoil axis.

5.2. FLUKA

FLUKA is a versatile general purpose Monte Carlo code that enables calculation of the yield of secondary particles and its transport. It has various nuclear reaction models built-in which allows the users to obtain the secondary particle yield and their angular distributions for several target-projectile combinations.

6. Results and discussion

The results from the experiment and from the calculations are shown in Fig. 7. The experimental data are shown as symbols, the results from the PACE code are shown as solid lines while the results from the FLUKA code are shown as broken lines. The plots have been artificially scaled for visual clarity. The statistical uncertainties in the experimental results are shown as vertical error bars. The experimental measurements in all the directions have a lower cutoff of ~1 MeV due to the threshold setting and the flight time.

The peak energy of the spectra obtained by experiments is about 3.5 MeV at 0° and 30° which then reduces to 2.5 MeV at 60° and to 1 MeV at 90° and 120°. Similar results from the PACE code shows higher value at 0° (by 1.5 MeV) but appears to agree well with the experimental data at other angles. The FLUKA calculations show lower values at all the emission angles. The slope of the spectra obtained from the PACE calculations approximately agree with the slopes of experimental data at all the emission angles, with minor deviations at the backward angles while the FLUKA code appears to predict similar slopes at all angles.

The energy differential yield obtained from the PACE and the FLUKA codes agree well with the experimental data in the forward angle but are higher by a factor of 2–3 at the backward angles. This can also be seen from Fig. 8, where the energy integrated neutron yields are shown. The experimental data agrees well with the PACE data in the extreme forward angle but is lower by a factor of 1.5–2.5 at all other angles. On the other hand, results obtained from the FLUKA code are higher by a factor of 4.5–1.5 with the maximum deviation observed at 0°.

The PACE code uses the Hauser–Feshbach [15] model to compute the emission from the compound nucleus. FLUKA on the other hand uses the Weisskopf–Ewing model [16] to do so. The resulting difference in the yield could be due to factors such as the fusion cross section, the level densities and the optical model parameters used in the two codes [3]. The slope of the measured and the calculated spectra grossly agrees with the experimental results. There is no indication of an appreciable change in the slope at higher energies that might have indicated the presence of pre-equilibrium emissions. Since the emissions calculated by the codes are from the compound nucleus only, the emission from this system appears to be predominantly from the compound nucleus formation and its subsequent statistical decay through various channels.

The neutron spectra reported here can be used to estimate the unshielded dose rate at unit distance at various angles, for the reaction and energy considered here. From the radiation protection point of view, the discrepancy in the results obtained by the various techniques as discussed could lead to an over estimation of the neutron ambient dose equivalent, when the double differential yield is calculated by the PACE and the FLUKA codes.

7. Conclusion

The thick target neutron yield and its angular distribution measured for 115 MeV ^{12}C projectiles incident on thick ^{27}Al target shows a forward peaking that is not reproduced by the PACE or the FLUKA codes. The shapes of the spectra given by these codes agree grossly at all angles but reasonably well in the forward angles. The peak energies predicted by the codes match reasonably well at the forward angles. The energy differential yields from PACE and the FLUKA code grossly agrees well with the experimental data in the forward angles but are higher at the backward angles.

Potential conflict of interest

None.

References

[1] P.K. Sarkar, Radiation Measurements 45 (10) (2010) 1476.
[2] C. Sunil, A. Saxena, R.K. Choudhury, L.M. Pant, Nuclear Instruments and Methods in Physics Research, Section A: Accelerators, Spectrometers, Detectors and Associated Equipment 534 (3) (2004) 518.
[3] C. Sunil, M. Nandy, P.K. Sarkar, Physical Review C: Nuclear Physics 78 (6) (2008), art. no 064607.
[4] M. Nandy, T. Bandyopadhyay, P.K. Sarkar, Physical Review C: Nuclear Physics 63 (3) (2001) 346101.

[5] Kazuo Shin, Kagetomo Miyahara, Tanabe, Eiji, Yoshitomo Uwamino, Nuclear Science and Engineering 120 (1) (1995) 40.
[6] C. Sunil, T. Bandyopadhyay, M. Nandy, V. Suman, S. Paul, V. Nanal, R.G. Pillay, P. K. Sarkar, Nuclear Instruments and Methods in Physics Research, Section A: Accelerators, Spectrometers, Detectors and Associated Equipment 721 (2013) 21.
[7] ⟨http://www.nndc.bnl.gov/exfor/exfor.htm⟩, last accessed 14 July 2015.
[8] A. Ferrari, P.R. Sala, A. Fasso, J. Ranft, FLUKA: A Multiple Particle Transport Code CERN-2005-10, 2005.
[9] G. Battistoni, F. Cerutti, A. Fassò, A. Ferrari, S. Muraro, J. Ranft, S. Roesler, P. R. Sala, AIP Conference Proceedings 896 (2007) 31–49.
[10] A. Gavron, Statistical model calculations in heavy ion reactions, Physical Review C 21 (1) (1980) 230.
[11] M. Cavinato, E. Fabrici, E. Gadioli, E. Gadioli Erba, G. Riva, Nuclear Physics A 679 (3–4) (2001) 753.
[12] ⟨http://www.srim.org/⟩., last accessed 1 June 2015.
[13] A. Pantaleo, L. Fiore, G. Guarino, V. Paticchio, G. D'Erasmo, E.M. Fiore, N. Colonna, Nuclear Instruments and Methods in Physics Research A 291 (3) (1990) 570.
[14] T. Kurosawa, N. Nakao, T. Nakamura, H. Iwase, H. Sato, Y. Uwamino, A. Fukumura, Physical Review C: Nuclear Physics 62 (4) (2000) 446151.
[15] W. Hauser, H. Fesbach, Physical Review 87 (1952) 366.
[16] V.F. Weisskopf, D.H. Ewing, Physical Review 57 (1940) 472.